Reprinted from:
Proceedings EUSAR 2004. May 25-27
p. 799-802

GROUND MOVING TARGET PARAMETER ESTIMATION FOR TWO-CHANNEL SAR

C. H. Gierull and I. Sikaneta

Defence R&D Canada – Ottawa
Radar Systems Section
3701 Carling Ave., Ottawa, ON, Canada, K1A 0Z4
E-mail: christoph.gierull@drdc-rddc.gc.ca

ABSTRACT

This paper introduces and analyses the performance of different techniques to estimate the parameters of ground moving targets in multi-channel SAR data. Candidates are filter-banks, the interferometric phase and direction-of-arrival estimation methods, which can work in either the raw data or in the compressed SAR image domain. Of particular interest are systems with only two channels because many existing or near-future SAR systems, such as RADARSAT-2, are restricted to a maximum of two sub-apertures. Desired parameters are the two velocity components (along- and across-track) and the true location. The results are evaluated with experimental airborne SAR data.

1 INTRODUCTION

In many civilian and military applications of airborne and spaceborne SAR imaging, it is highly desirable to simultaneously monitor ground traffic. The measurement of object motion using SAR requires two consecutive operations. Firstly, the detection in the SAR data and, secondly, target parameter estimation such as of location, speed and trajectory. Target detection and estimation can either be performed incoherently with a single SAR sensor, or coherently, with much higher fidelity, with two or more apertures. While many authors have investigated the detection part in the past, the estimation problem has been rarely dealt with, e.g.[1].

Great importance is attached to the practical applicability of the presented techniques, particularly with regard to the experimental MTI-mode of RADARSAT-2 [2]. The techniques presented in this paper are analysed with real data acquired during an experiment conducted at Canadian Forces Base (CFB) Petawawa on 14 July 1999. The SAR data were acquired by the Environment Canada CV 580 C-band SAR configured in its Along-Track Interferometric (ATI) mode [3].

Figure 1 shows a SAR image of the test site including the analysed part of Highway 17 (second box from top). This site was comprised of composite terrain containing a part of a highway, forests and areas with shrubby vegetation. Note, no fast moving vehicles are recognizable on or nearby the highway, even though approximately ten different cars and trucks were traveling on that road during the observation period. Processing two SAR images with ATI for slow moving vehicles, that are still focused but displaced, has been proven to work successfully in that a slowly moving control vehicle was detected [4].

2 MOVING TARGET DETECTION

The first step in any MTI mode is the actual test for presence of movers in the measured data. In air-to-ground ap-

Figure 1: *SAR image of Petwawa from 14 July 1999 along with selected areas used to verify the theoretical analysis.*

plications, such as SAR, this task is challenging because of the simultaneously overlayed clutter power, which can, in the mainbeam regions of the antenna pattern, be a multiple of the signal power. Since the clutter must be suppressed prior to target testing over the entire clutter Doppler spectrum, one-channel based techniques are typically very limited in performance. Although, real multi-channel SAR-GMTI is known to enhance the detection and estimation performance drastically [5], many present and also future radar systems are and will be restricted to only two parallel receiver channels due to limited resources. This is particularly true for space-based sensors, such as upcoming RADARSAT-2 and TerraSAR-X.

Ground Moving Target Detection (GMTD) can be either achieved in the raw data domain, i.e. without actually focussing/compressing the data in along-track (azimuth direction) or it can be done on the processed data, i.e. in the image domain [6, 7]. Either domain has its advantages and disadvantages. While raw data techniques usually suffer from low SNR they usually allow detection of targets in a much wider velocity range than image-based techniques. This is due to the smearing effects of the point spread function for fast moving targets when they are filtered with the optimum filter for the stationary world during SAR processing, e.g. [3].

For the subsequent moving target parameter estimation it is assumed in this paper that the detection has been done in the raw data domain, as described in [6]. However, if found that the SNR is too low in the raw data, the detection may be done after compression/focusing and the entire corresponding range line (in which the target was detected)

could be analysed as described below. In this approach the entire azimuth interval is segmented into small, typically highly overlapping, pieces, where the data of each segment are successively analysed for movers. The data segment is transformed into the Fourier or Doppler domain; the length of the segment is chosen so that a moving target is confined to one Doppler cell, see Fig. 2 in [6]. The adequate CFAR thresholds are now applied to each range-Doppler data segment separately and the results are stored in lists. Recently, several new metrics for two channel SAR-GMTD

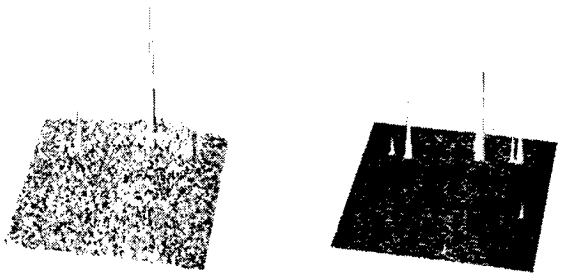

Figure 2: *Demonstration of the reduction of false alarms through the additional detector step.*

have been proposed and compared to well known techniques [8], such as Along-Track Interferometry (ATI) and Displaced Phase Centre Antenna (DPCA) [10, 9]. The most promising group of methods, are two-step detectors also called hyperbolic detectors. These are based on the combination of two independent metrics in such a way that the first metric detects targets with a high probability of detection while allowing a rather large number of false alarms. Applying the second metric to only the alarms which passed the first detection step ought to decrease the number of false alarms while preserving the probability of detection. Using DPCA as the primary detector typically results in many false alarms particularly in very heterogeneous terrain such as urban areas. This is due to the presence of many very strong point-like stationary scatterers which are after clutter suppression (i.e. subtraction of the two channels) still so strong that they exceed the detection threshold. Knowing that stationary targets are typically suppressed much more than moving targets, it is possible to apply a second test which only retains those detections with a relatively small amplitude change before and after suppression.

An example of the impact of such a second step is illustrated in the range-Doppler plot in Fig. 2 for one segment of the highway sub-scene. The left side shows the DPCA magnitude, where the clutter power is still relatively high compared to some small RCS targets in the front. Applying the second step now reveals the small or low-speed targets. The peaks in the back part of the plot are various fast targets traveling on the highway.

3 DETECTION TRACK ARBITRATION

One particular problem faced by any MTI technique is the clustering of individual detections to target tracks. The conceived algorithm starts with detections at the far left side in Fig. 3 and checks whether adjacent range cells for the next time sample contain a detection as well. If positive, both are assigned a common target track ID and the next pixels to the right are checked until no direct neighbour includes a detection anymore. At this point, this specific ID expires and the track ID counter is incremented by one. After reaching the right end of the scene only those tracks are kept whose number of detections exceeds a predefined value. This value is based on physical parameters such as antenna beamwidth and a range for reasonable target speeds. The corresponding Doppler histories, Fig. 4,

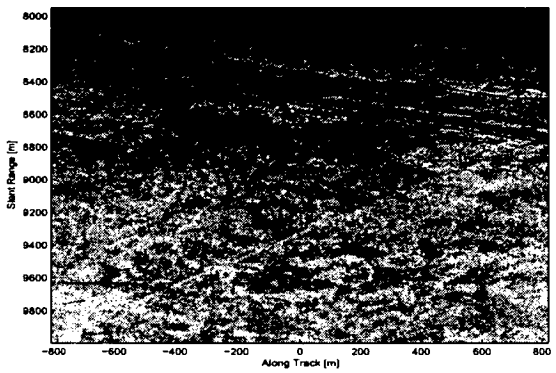

Figure 3: *Slant range positions along slow time.*

can be used to further eliminate more false alarms, for instance, by rejecting all those tracks which do not follow an allowed Doppler-time trajectory, e.g. the pixel clusters at roughly -225 Hz on the left side of the plot.

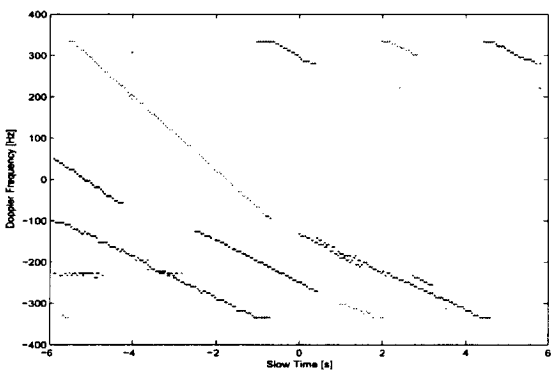

Figure 4: *Doppler frequency estimates along slow time.*

4 TARGET PARAMETER ESTIMATION

4.1 SIGNAL MODEL

The parameters describing the moving target, such as velocity in along-track direction v_x, velocity in across-track or range direction v_y and its location x_0 at time $t = 0$ are combined in the vector $\boldsymbol{\xi} = [v_x, v_y, x_0]^T$. Alternatively, the position x_b, when the platform is broadside to the target can be used as the location parameter. This position depends on the time t_b, which depends on the aircraft velocity v_a:

$$t_b = -\frac{x_0}{v_x - v_a} \quad \text{or} \quad x_b = v_a t_b = -\frac{v_a}{v_x - v_a} x_0. \quad (1)$$

It is evident that both positions are identical for stationary scatterer with $v_x = 0$. Note that the range-position y_0 is assumed to be known because of the range-resolution of

the radar. The far-field model for the received target signals is

$$\boldsymbol{s}(t,\boldsymbol{\xi}) \;=\; a e^{-j2\beta R(t,\boldsymbol{\xi})} \begin{bmatrix} D_1(u(t,\boldsymbol{\xi})) \\ D_2(u(t,\boldsymbol{\xi})) e^{j\beta u(t,\boldsymbol{\xi}) d} \end{bmatrix} \quad (2)$$

where a is the complex amplitude describing the reflectivity of the scatterer, $R(t,\boldsymbol{\xi})$ denotes the slant range distance to a reference channel and $u(t,\boldsymbol{\xi})$ is the directional cosine from the reference antenna to the moving target on the ground. $D_i(u)$ describes the two-way antenna pattern of the ith channel and $\beta = 2\pi/\lambda$ is the wavenumber. Without accelerations the distance can be expressed as

$$R(t,\boldsymbol{\xi}) = \sqrt{(x_0 + (v_x - v_a)t)^2 + (y_0 + v_y t)^2 + H^2}. \quad (3)$$

For small antenna azimuth beamwidths, i.e., a relatively small period of time in which a particular scatterer is 'seen' by the radar, it is possible to approximate (3) by a second order Taylor series around broadside-time t_b:

$$\begin{aligned} R(t) &\cong R(t_b,\boldsymbol{\xi}) + R'(t_b,\boldsymbol{\xi})(t-t_b) + \frac{R''(t_b,\boldsymbol{\xi})}{2}(t-t_b)^2 \\ &= R_b + v_s(t-t_b) + \frac{v_{\mathrm{rel}}^2}{2R_b}(t-t_b)^2, \end{aligned} \quad (4)$$

where $v_s = \alpha v_y, v_{\mathrm{rel}}^2 = (v_x - v_a)^2 + (1-\alpha^2)v_y^2, \alpha = y_b/R_b$, and the broadside distance can be expressed as $R_b = \sqrt{(y_0 - v_y t_b)^2 + H^2} = \sqrt{y_b^2 + H^2}$. The point of closest approach t_c, where the Doppler frequency vanishes can be determined via $R'(t_c,\boldsymbol{\xi}) = 0$ to

$$t_c = t_b - v_s R_b / v_{\mathrm{rel}}^2. \quad (5)$$

Note, the position $x_c = t_c v_a$ is the displaced location in azimuth where the moving target appears in the conventionally processed SAR image.

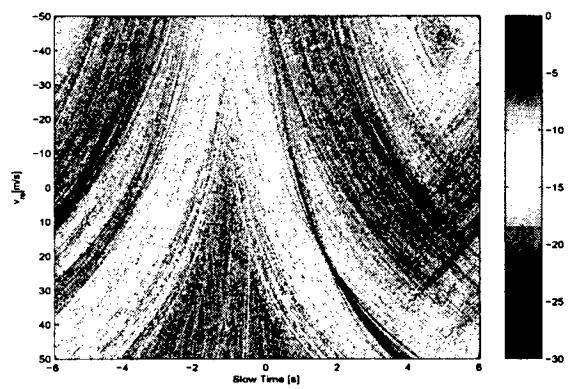

Figure 5: *Normalized amplitude [dB] of along-track matched filter response of aft channel.*

4.2 PARAMETER FIT

A simple but not very reliable estimation scheme is to utilize the range walk of the individual tracks (if any are present), i.e. to apply a direct parameter fit of equation (4) to the detected range-time trajectories, Fig. 3. Since this technique is solely based on range information (resolution) it is not sufficiently accurate but these initial estimates can, however, be used to resolve phase ambiguities, such as the correct sign for v_y, i.e. approaching or receding target.

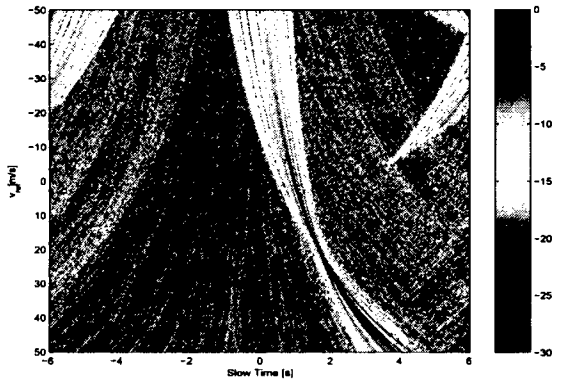

Figure 6: *Normalized amplitude [dB] of along-track matched filter response of channel difference (DPCA).*

4.3 MATCHED FILTER BANKS

Estimation of the **along-track velocity** component v_x can be achieved by applying a matched filter bank $r(t,\boldsymbol{\xi}') = \exp(-2j\beta R(t,\boldsymbol{\xi}'))$ with variable parameter vector $\boldsymbol{\xi}' = [v_{\mathrm{rel}}', v_s' = 0, t_b' = 0]^T$ to the individual target tracks (Maximum-Likelihood Estimator (MLE)). Fig. 5 shows the matched filter responses for the dark blue highway track (@ 8500 m roughly in the center of Fig. 3), where v_{rel}' was varied between -50 and 50 m/s. Even though the maximum appears at a reasonable velocity of $\hat{v}_{\mathrm{rel}}$=22.7 m/s, the clutter contamination within the data can clearly be seen. The time at which the maximum occurs, represents the closest approach of platform and target $t_c = 1.95$ s. Around the the optimum v_{rel} the matched filter responses shift away from t_c and broaden; the ridge is tilted and fans out at the edges. These effects are caused by the mismatch of v_s in the matched filter and the data.

After co-registration, i.e. the time shift of the aft channel by $d/(2v_a)$ [11], the DPCA difference of the two channels can be written as

$$p(t,\boldsymbol{\xi}) = 2ja \sin(\beta g(t,\boldsymbol{\xi}))\, e^{-2j\beta R(t,\boldsymbol{\xi})} e^{-j\beta g(t,\boldsymbol{\xi})}, \quad (6)$$

where $g(t,\boldsymbol{\xi}) = v_s d/(2v_a) + e(\boldsymbol{\xi})(t-t_b)/2$ with

$$e(\boldsymbol{\xi}) = \frac{v_{\mathrm{rel}}^2 d}{R_b v_a} + \frac{(v_x - v_a)}{R_b} d. \quad (7)$$

Therefore, $p(t,\boldsymbol{\xi})$ is of identical structure as either channel signal but with the stationary clutter components significantly suppressed. Applying the matched filter bank onto the DPCA output results in Fig. 6, where a clutter amplitude suppression of about 10-15 dB can be recognized.

Analogously, a **matched filter bank for the across-track velocity** component v_s can be used, now with varying parameter vector $\boldsymbol{\xi}' = [\hat{v}_{\mathrm{rel}}, v_s', 0]^T$. In order to avoid ambiguous impulse responses the length of the reference function should not exceed the length of the target trajectory. Fig. 7 shows the filter bank map where v_s' is varied from -10 to 10 m/s with the maximum of $\hat{v}_s = 3.85$ m/s at time $t_b = -0.825$ s, which is in fact identical to broadside time (provided the track is perfectly centered around t_b). Inserting this MLE, i.e. $\hat{v}_s$, into the reference function and repeating the v_{rel} matched filter bank results in Fig. 8. The ridge is now correctly shifted to the broadside time t_b

and also straightened out. One can mathematically show that the center of the impulse response is independent of a varying mismatch in v_{rel} as long as $v_s' - v_s = 0$, i.e. the correct v_s has been included in the reference function. This property can be utilised in an **adaptive estimation scheme** which varies v_s' until the fan in the v_{rel} matched filter map is straightened. As one can see, the estimated velocity $\hat{v}_s$ is directly coupled to the broadside time estimate $\hat{t}_b$; small errors in $\hat{v}_s$ usually translate into relatively large position errors $\hat{x}_b$, particularly for spaceborne systems (because the time must be multiplied with the platform speed v_a).

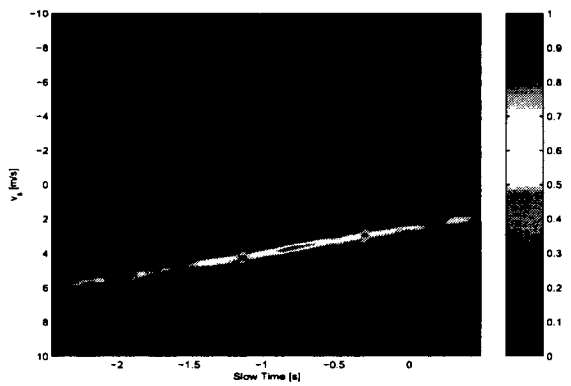

Figure 7: *Normalized amplitude of across-track matched filter response of channel difference (DPCA).*

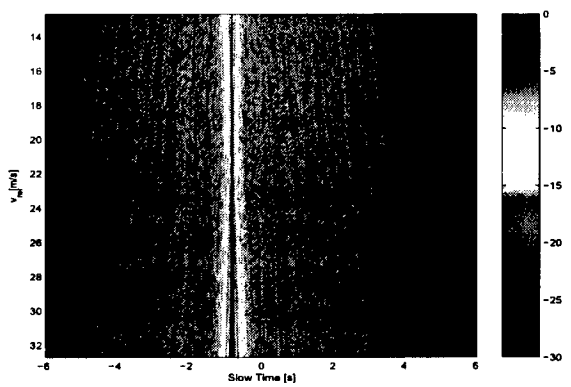

Figure 8: *Normalized amplitude [dB] of along-track matched filter response of channel difference (DPCA) after insertion of estimate $\hat{v}_s$.*

A multi-channel SAR overcomes this shortfall by adding additional degrees of freedom to the estimation process. Here, the angle $u(t, \boldsymbol{\xi})$ can be independently estimated by beamforming techniques to reveal the target position [5]. These **direction-of arrival (DOA) estimators** cannot directly be applied to two-channel SAR systems since only one degree of freedom is left after clutter suppression, e.g. via DPCA. However, using known STAP techniques such as PRI-staggering to increase the overall time-space dimensionality allows (to a certain degree) the DOA estimation capability of a two-channel SAR to be preserved even after clutter suppression. These techniques are currently under investigation.

4.4 ATI PHASE

Beside matched filter banks there also exists the possibility to estimate the velocity v_s from the interferometric phase ϕ after compression of the target trajectory with the optimum estimate $\hat{v}_{\text{rel}}$ and $v_s' = 0$. Using the first order Taylor series expansion of the directional cosine

$$u(t, \boldsymbol{\xi}) = \frac{x_0 + (v_x - v_a)t}{R(t, \boldsymbol{\xi})} \simeq \frac{v_x - v_a}{R_b}(t - t_b), \qquad (8)$$

the ATI phase at $t = t_c$ can be calculated to

$$\phi(\boldsymbol{\xi}) = \frac{\beta d}{2}\left(\frac{1}{v_a} - \frac{(v_x - v_a)}{v_{\text{rel}}^2}\right) v_s + \frac{\beta e(\boldsymbol{\xi})}{2}\delta t, \qquad (9)$$

where $\delta t = (T_u + T_l)/2 - t_b$ describes the deviation of the target trajectory center from broadside time. T_l and T_u denote the start time and end time of the target track. Taking for instance the maximum phase value in Fig. 9, $\hat{v}_s$ can be estimated by solving the two equations (9) and (4), provided that the track is perfectly centered around t_b, i.e. $\delta t = 0$.

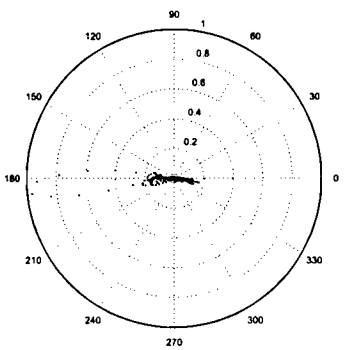

Figure 9: *Along-track interferometric phase.*

5 REFERENCES

[1] Ender. J., "Azimutpositionierung bewegter Ziele mit Mehrkanal-SAR", *U.R.S.I. Jahrestagung (Kleinheubacher Berichte)*, vol. 38, pp. 749–758, Oct. 1994.

[2] Gierull, C. H. and Livingstone, C., "SAR-GMTI Concept for RADARSAT-2," *in The Applications of Space-Time Processing*, Edt. Klemm, R., IEE Press, Stevenage, UK, 2004.

[3] Livingstone, C., Sikaneta, I., Gierull, C. H., Chiu, S., Beaudoin, A., Campbell, J., Beaudoin, J., Gong, S. and T. Knight, "An airborne SAR experiment to support RADARSAT-2 GMTI," *Canadian J. Remote Sensing*, vol. 28, no. 6, pp. 1–20, Dec. 2002.

[4] Gierull, C. H., "Statistical Analysis of Multilook SAR Interferograms for CFAR Detection of Ground Moving Targets," *IEEE Trans. Geosci. Remote Sensing*, vol. 42, 2004.

[5] Ender, J. H. G., "Space-Time Processing for Multichannel Synthetic Aperture Radar," *IEE Electr. and Comm. Eng. J.*, pp. 29–38, 1999.

[6] Gierull, C. H. and Sikaneta, I., "Raw Data Based Two-Aperture SAR Ground Moving Target Indication," *Proc. of IGARSS'03*, Toulouse, France, 2003.

[7] Meyer-Hilberg, J., Bickert, B. and Schmid, J., "Flight Test Results of a Multi-Channel SAR/MTI Real-Time System," *Proc. EUSAR'02*, pp. 209-212, 2002.

[8] Sikaneta, I., Gierull, C. H. and and Chouinard, J.-Y., "Metrics for SAR-GMTI based on Eigen-Decomposition of the Sample Covariance Matrix," *Proc. Int. RADAR 2003*, Adelaide, Australia, 2003.

[9] Stockburger, E. F. and Held, D. N., "Interferometric Moving Ground Target Imaging," *Proc. IEEE Radar Conf.*, pp. 438–443, 1995.

[10] Gierull, C. H., "Moving Target Detection with Along-Track SAR Interferometry," *Defence Research & Development Canada - Ottawa. (Technical Report TR 2002-084)*, 2002.

[11] Sharma, J., "The influence of target acceleration on parameter estimation and focusing in SAR imagery" *Master Thesis, University of Calgary*, Canada, 2004.

#522075

CA024497